VISUALISATION AND QUANTIFICATION OF WIND-INDUCED VARIABILITY IN HYDROGEN CLOUDS FOLLOWING RELEASES OF LIQUID HYDROGEN

Palin, I.[1], Lyons, K.[2], Buttner, W.[1], Coldrick, S.[2], Hall, J. E.[2], Atkinson, G.[2], Thorson, J.[1] and Royle, M.[2]

[1] Energy Conversion and Storage Systems Center, National Renewable Energy Laboratory, 15013 Denver West Parkway, Golden, CO 80401-3305

[2] Major Hazards, Science Division, Health and Safety Executive, Harpur Hill, Buxton, Derbyshire, SK17 9DZ, UK

Kieran.Lyons@HSE.gov.uk; William.Buttner@NREL.gov

ABSTRACT

Well characterized experimental data for consequence model validation is important in progressing the use of liquid hydrogen as an energy carrier. In 2019, the Health and Safety Executive (HSE) undertook a series of liquid hydrogen dispersion and combustion experiments as a part of the Pre-normative Research for Safe Use of Liquid Hydrogen (PRESLHY) project. In partnership between the National Renewable Energy Laboratory (NREL) and HSE, time and spatially varying hydrogen concentration measurements were made in 25 dispersion experiments and 23 congested ignition experiments associated with PRESLHY WP3 and WP5, respectively. These measurements were undertaken using the hydrogen wide area monitoring system developed by NREL. During the 23 congested ignition experiments, high variability was observed in the measured explosion severity during experiments with similar initial conditions. This led to the conclusion that wind, including localized gusts, had a large influence on the dispersion of the hydrogen, and therefore the quantity of hydrogen that was present in the congested region of the explosions. Using the hydrogen concentration measurements taken immediately prior to ignition, the hydrogen clouds were visualized in an attempt to rationalize the variability in overpressure between the tests. Gaussian process regression was applied to quantify the variability of the measured hydrogen concentrations. This analysis could also be used to guide modifications in experimental designs for future research on hydrogen combustion behavior.

1.0 INTRODUCTION

1.1 Project Background

The use of liquid hydrogen (LH2) as an alternative energy carrier to fossil fuels could see wider adoption in various industries with the aim of decarbonization. In particular, this could include various transportation sectors, such as road, rail, and aviation. To enable the safe adoption of LH2, the Pre-normative Research into the Safe Use of Liquid Hydrogen (PRESLHY) project [1] was conducted. The objectives of this project were to identify and study poorly understood and highly hazardous scenarios relating to the use of LH2. To this end various theoretical, numerical, and experimental activities were undertaken by an international consortium, which resulted in a handbook on LH2 safety [2] and recommendations for regulations, codes, and standards [3].

As a part of this project, the Health and Safety Executive UK (HSE) undertook a series of LH2 releases investigating phenomena relating to dispersion and electrostatics [4], and combustion [5]. The experiments were conducted on a 32 m diameter pad at the HSE Science and Research Centre, UK, with an LH2 road tanker as the hydrogen source with flow rates of up to 300 g/s.

A consistent observation was the large effect that wind conditions had on the dispersion of the releases, resulting in modeling the variability experimental outcomes [6]. Figure 1 shows two stills from drone footage of the same experiment demonstrating the dependence of the far-field dispersion on the ambient conditions.

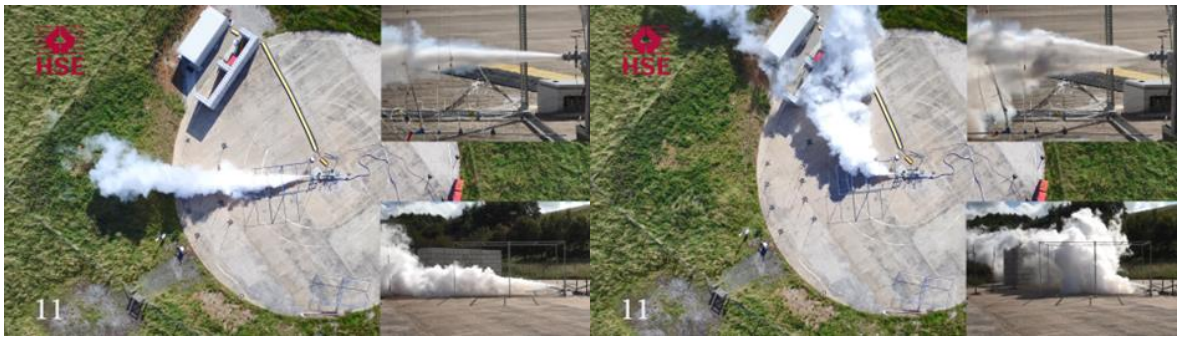

Figure 1: Stills from video taken during dispersion test 11 showing co-flow (left) and cross-flow (right) wind conditions

This variation had a particular influence on the combustion experiments, in which one ignition event with identical initial conditions to another resulted in a much more severe explosion, with peak overpressures of 120 kPa compared to 12 kPa.

In this paper hydrogen concentration measurements made during the combustion experiments were used to visualize the hydrogen clouds prior to ignition. From these visualizations, the mass of hydrogen involved in the explosion events will be estimated, allowing for an assessment of explosion severity using the overpressure measurements. The assessments will be compared to typical gas explosion behavior to demonstrate the legitimacy of the mass estimation method in generating quantitative results.

1.2 HyWAM System Overview

Hydrogen Wide Area Monitoring is defined as the quantitative or qualitative 3-dimenstional spatial and temporal profiling of intended or unintended hydrogen releases. The NREL HyWAM is based upon an array of hydrogen sensors connected to remote sampling points (SP) distributed around a hydrogen facility to profile hydrogen dispersions following releases. Sample gas is continuously transported from the SPs to the remote hydrogen sensors via pneumatic lines. It was originally developed to characterize outdoor cold hydrogen plume behavior following venting of liquid hydrogen (LH2) [7]. The NREL Sensor Laboratory supported HSE during their LH2 releases performed under the auspices of PRESLHY [8] program by providing a 32-point HyWAM System. The NREL HyWAM used thermal conductivity hydrogen sensors that have a range of 0 to 100 vol% H_2 and a lower detection limit of approximately 0.1 vol% with a response time (t_{90}) of 250 ms, making it an ideal platform for profiling the cold hydrogen releases performed by HSE. Results of LH2 profiling performed under PRESLHY WP3 were presented earlier [9,10,11]. To support HSE work on PRESLHY WP5 a 16-measurement point HyWAM was reconfigured in the congestion cage to profile hydrogen concentrations during and following ignition [12].

1.3 Summary of Previous Work

The experimental setup and key findings have been previously reported [5] [13] and the full data outputs are publicly available [14], but the following summary provides context for the activities undertaken in the upcoming analysis.

A total of 23 ignited LH2 releases were conducted. In each case, the hydrogen was released into a frame providing congestion, analogous to a system of pipework that could occur at a refueling station or similar infrastructure. The release nozzle diameter and storage pressure of the LH2 were altered, effectively resulting in 6 different mass flow rates. The congestion level was also changed between two volume blockage ratios: <1.5% and >4%. Table 1 shows a summary of the initial conditions for each test, as well as some key measurements. Table 3 shows the wind speed and direction measurements taken at the release point (local) and 16 m from the release point (far-field). The measurements of wind direction

near the release point were limited to cardinal directions while the far field measurement provided degree level resolution.

Table 1: Summary of initial conditions and overpressure results from the congested ignition LH2 experiments.

Trial No.	Orifice size (mm)	Tanker P (kPa)	Congestion level	P max location	P max 6.5 m (kPa)	P max 11.5 m (kPa)	P max (kPa)
1	6	100	<1.5%	Centre	0.2	0.1	1
2	12	100	<1.5%	Side	4.0	2.3	52
3	25.4	100	<1.5%	Rear	0.5	0.4	16
4	12	100	<1.5%	Rear	1.2	0.7	3
5	25.4	100	<1.5%	Rear	1.1	0.5	2
6	12	100	<1.5%	Rear	1.2	0.7	4
7	25.4	100	<1.5%	Rear	0.7	0.4	38
8	12	100	<1.5%	Centre	1.4	0.8	7
9	12	100	<1.5%	Centre	1.0	0.5	4
10	25.4	100	<1.5%	Centre	0.4	0.2	1
11	6	500	<1.5%	Rear	1.3	0.7	14
12	12	500	<1.5%	Rear	4.0	2.5	39
13	12	500	<1.5%	Rear	5.0	3.0	13
14	12	500	<1.5%	Rear	2.0	1.2	53
15	12	500	<1.5%	Rear	4.0	2.0	10
16	12	500	<1.5%	Centre	4.0	2.0	55
17	12	500	<1.5%	Rear	3.0	1.5	67
18	25.4	500	<1.5%	Rear	1.5	0.7	4
19	25.4	500	<1.5%	Rear	7.0	4.0	15
20	6	100	>4%	Centre	0.3	0.2	1
21	12	100	>4%	Rear	4.0	2.5	15
22	12	100	>4%	Rear	6.5	4.0	13
23	12	100	>4%	Rear	47.0	20.5	128

Table 2: Calculation of mass flow in each event case.

Pressure (bar)	Nozzle diameter (mm)	Mass flow (g/s)
5	6	90-100
5	12	265
5	24	298
1	6	Unknown
1	12	104-107
1	24	135-144

Table 3: Average Wind speed and direction measurements taken locally and far-field.

Trial No.	Local 5 min average wind speed (m/s)	Local 5 min average wind direction	Far-field wind speed (m/s)	Far-field wind direction (°)
1	1.0	W	2.03	172
2	3.4	S	2.00	136
3	2.0	SW	0.52	224
4	2.7	SE	1.09	123
5	2.4	W	1.38	189
6	0.7	SE	1.44	107
7	1.7	SSE	1.62	122
8	2.0	W	2.58	266
9	2.0	W	3.74	243
10	2.0	N	2.62	250
11	1.0	NE	1.01	127
12	0.7	SE	1.44	45
13	1.0	NW	1.01	139
14	1.0	NE	2.48	79
15	2.4	NE	2.14	42
16	2.7	N	1.24	299
17	0.7	N	0.69	312
18	0.7	SE	0.60	70
19	0.7	E	1.21	179
20	2.0	E	1.37	94
21	1.4	SE	2.70	85
22	2.4	E	2.14	50
23	2.0	E	3.22	71

Temporal hydrogen concentrations were measured at 16 points in the congestion frame at a sampling rate of 1 measurment every 300 ms. Following ignition (from a stage pyrotechnic) overpressure measurements were made at 3 points inside the frame, and 5 outside the frame. The measurements of particular relevance are those made at 6.5 m and 11.5 m.

The results showed that an increased hydrogen inventory released could result in stronger events upon ignition. However, it was proposed that other effects such as mixing also influenced the post-ignition behavior. A severe event was only observed in one case with the high level of congestion. This could not be attributed to a change in the initial conditions, as other identical tests did not result in the severe event. A qualitative assessment suggests that a counter-flow gust contributed to this outcome.

The objective of this paper is to use the hydrogen concentration measurements taken prior to ignition to visualize and quantify the hydrogen cloud within the congestion frame. In doing so, the variability in post-ignition behavior could be better explained, and therefore enable more accurate predictions of explosion severity based on hydrogen concentration measurements.

2.0 METHODS

The broad method used for this analysis is to:

- identify the relevant tests and measurements to use,
- use the hydrogen concentration measurements to create a three-dimensional visualization of the hydrogen cloud,
- estimate the mass of hydrogen within the congestion frame based on the visualizations,
- predict the overpressures from an explosion with the mass of hydrogen predicted,
- compare the predicted overpressures to the measured values.

A quantitative description in the variability of hydrogen concentration is also offered.

2.1 Concentration Visualization and Quantification Technique

Visualizing data validates the sensors' response to the presence of hydrogen by showing that it could reasonably be produced by a gas plume. In order to visualize the data, gaussian process (GP) regression, a machine learning spatial interpolation method, was implemented. Typically referred to as kriging, GP was first used in mining to estimate concentrations of resources from isolated samples and has since seen use in many disciplines [16]. Spatial interpolation is the process of obtaining quantitative estimates of process values at unobserved locations based on observed locations and process characteristics [17]. Kriging analysis is dependent on knowledge of the variogram, or function describing the spatial dependance of a stochastic process. For this analysis we assume our data follows a gaussian spatial dependance giving the variogram as follows [18].

$$\boldsymbol{P}\cdot\left(\mathbf{1}-\boldsymbol{e}^{-\left(\frac{\boldsymbol{d}^{2}}{\left(\frac{4}{7}\boldsymbol{r}\right)^{2}}\right)}\right)+\boldsymbol{n} \qquad \textbf{(1)}$$

Here, P is the partial sill (sill – nugget), d is the distance value where the variogram is to be calculated, r is the range and n is the nugget. The range is considered the distance between data at which the variance is no longer corelated. The sill is the value the variogram approaches as data becomes uncorrelated. The nugget is the allowable variance between points at the same spatial coordinates and is representative of the error in the data. A graphical representation of the parameters is shown in Figure 2.

The use of this methodology was motivated by the unexplained variability in explosion characteristics of tests with the same initial conditions, and by the need for less computationally expensive analytical techniques compared to computational fluid dynamics (CFD). CFD analysis has been performed on a similar data set from a series of dispersion experiments in the PRESLHY project and it was shown that wind contributes significantly to unpredictability of dispersion behavior [6]. Here, kriging is proposed as supplementary analysis for gas dispersion where CFD would be too computationally intensive to explain variability. Gaussian process regression was selected because gas dispersion is known to be a gaussian process and interpolation was needed to investigate concentrations outside the sensor array and between sensor points.

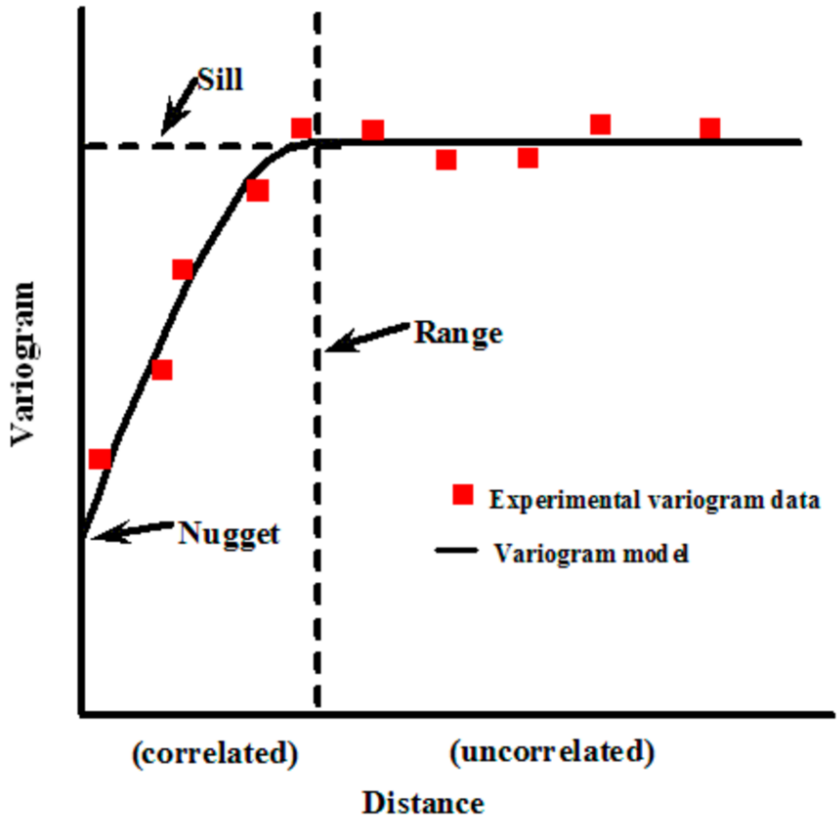

Figure 2: Graphical representation of Sill, Range, and Nugget provided by Interstate Technology Regulatory Council [19]

To achieve a quantitative result from a trial, the concentration value at each point in space produced by the kriging interpolation is assumed to be representative of the concentration in the surrounding cube with side lengths equal to the spatial resolution. Each cube therefore has a defined volume and hydrogen concentration. The volume percent concentration was then converted to total mass by using the ideal gas law assuming that the pressure in the gas cloud was equal to the ambient pressure and with the volume considered to be the reported volume percent of the volume in congestion cage. Then every point with a concentration above the lower flammable limit of hydrogen was summed to give the total flammable mass in the plume.

In order to choose parameters for the kriging process the optimize library from Scipy[1] was used. The parameters were tuned with the goal of optimizing the parameters such that they illuminated the strongest relationship between the kriging mass estimate and the maximum overpressure. To quantify the correlation between the two data sets we used the Spearman correlation coefficient. The Spearman correlation coefficient (ρ) ranges from -1 to 1 and is a measure of how well two data sets can be related by a monotonic function. If our data maintained perfect covariance, we would see a ρ of 1. We created a python function that takes the sill, range, and nugget as input, performs interpolation on every trial in the set, correlates the summations with the overpressure results, and returns the quantity (1-ρ). This makes the output range 0 to 2, with 0 being the most correlated. This allowed us to use

[1] https://scipy.org/ (accessed 31-03-2023)

Scipy's minimize function which varies the inputs of a function repeatedly, seeking the lowest possible output.

2.2 Explosion Severity Estimates

The vapor cloud explosions (VCEs) conducted during the experimental series were not accurately described in terms of TNT equivalence [5]. Overpressure measurements of the same event taken at different distances resulted in different estimates for TNT equivalent mass. As such, the TNO Multi Energy Method (MEM) [15] was used to validate the mass estimates.

The basis of the theory is the observation that blast effects are primarily generated in VCEs that are sufficiently obstructed or confined. As such, in the case of these experiments it is assumed that only the hydrogen contained within the congestion frame will contribute significantly to the overpressures generated. The severity of the explosion is then assigned a severity between 1 and 10.

Using the mass of the hydrogen within the cloud, estimated with the visualization method, the scaled distance *r'* will be determined at two locations: 6.5 m and 11.5 m using equation 2. These distances are where the furthest overpressure measurements from the center of the congestion frame were made. Since the actual location of ignition is unknown in each case, the larger distances enable a higher proportional certainty in analysis.

$$r' = \frac{r}{\left(\frac{M_{H2}\, LHV_{H2}}{P_a}\right)^{\frac{1}{3}}} \tag{2}$$

Where *r'* is the scaled distance; *r* is the radial distance from the center of the explosion, taken as 6.5 m and 11.5 m; M_{H2} is the mass of hydrogen inside the congested region in kg; LHV_{H2} is the lower heating value of hydrogen, taken as 120 MJ/kg; and P_a is the ambient pressure, taken as 96.9 kPa to account for Buxton altitude. The exact center of the explosion has uncertainties due to wind direction and ignition location. Therefore to reduce the error in the scaled distance, the overpressure measurements taken furthest from the congestion cage were used.

In a typical application of the MEM, the overpressure estimates are then derived by assigning a TNO level between 1 and 10, then read from the peak side-on overpressure pressure graph. This graph is shown in the results and discussion section in figure 7. Assigning the severity is an uncertain task, which has a large effect on the estimated pressure. To limit the impact of a subjective and arbitrary selection on the validation work, the TNO level will be assigned using the overpressure measurements and the *r'* value estimates. If the points on the graph for 6.5 m and 11.5 m show agreement with the predicted trend, the TNO level will be taken as a reasonable approximation of the event.

3.0 RESULTS AND DISCUSSION

3.1 Flammable Cloud Visualizations

By observing the plots produced from a kriged trial in conjunction with the video recordings some qualitative conclusions about the technique can be made. As can be seen in the images below, the GP regression yields a better representation of the low momentum dispersive characteristics of the plume than the high momentum release jet characteristics. These plots show that the higher density plume, above the lower flammable limit, maintains a similar shape across the trials but that counter flow wind and congestion contribute significantly to the accumulating density of hydrogen. In the plots, generated by the python library matplotlib, the units on figures 3 through 6 are shown in decimeters giving ten spatial units per meter, and the blue dot at (60,80,10) shows the release point.

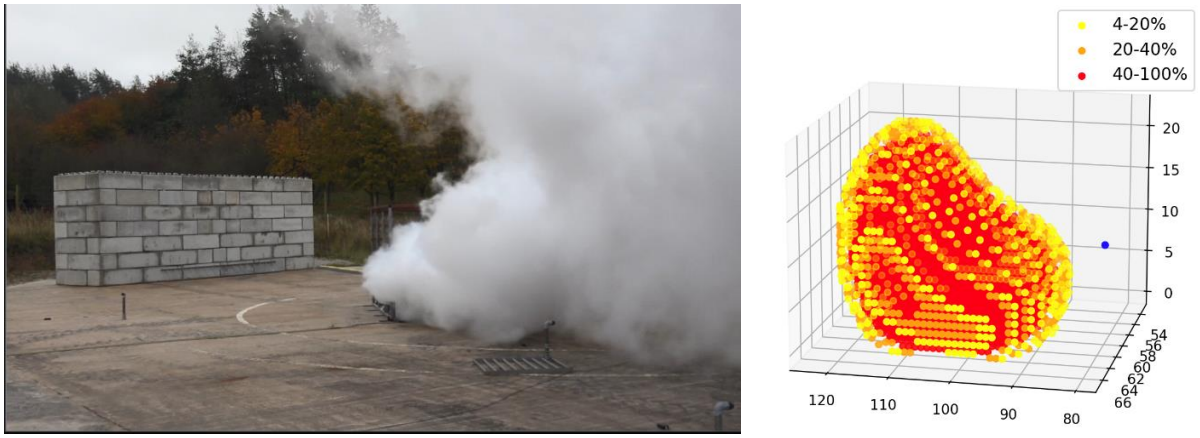

Figure 3: Photo and kriging plot of release event 2: low congestion, high counter flow wind

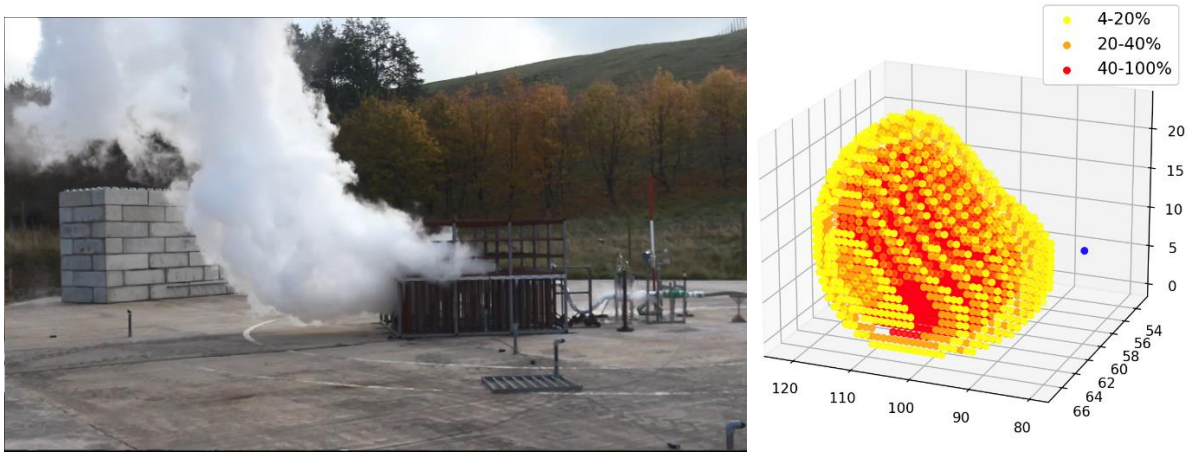

Figure 4: Photo and kriging plot of release event 4: low congestion, low counter flow wind

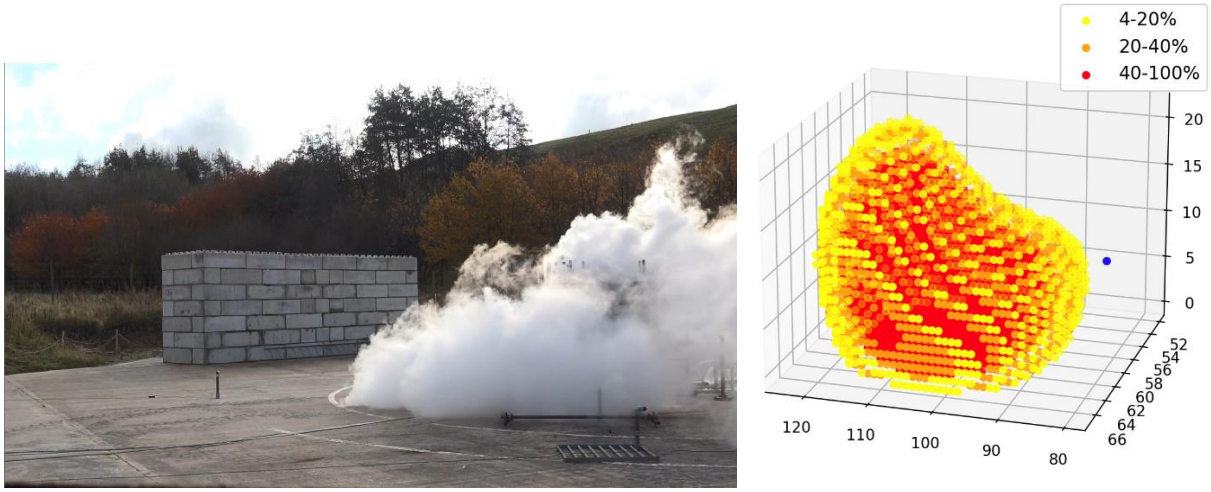

Figure 5: Photo and kriging plot of release event 21: high congestion, low counter flow wind

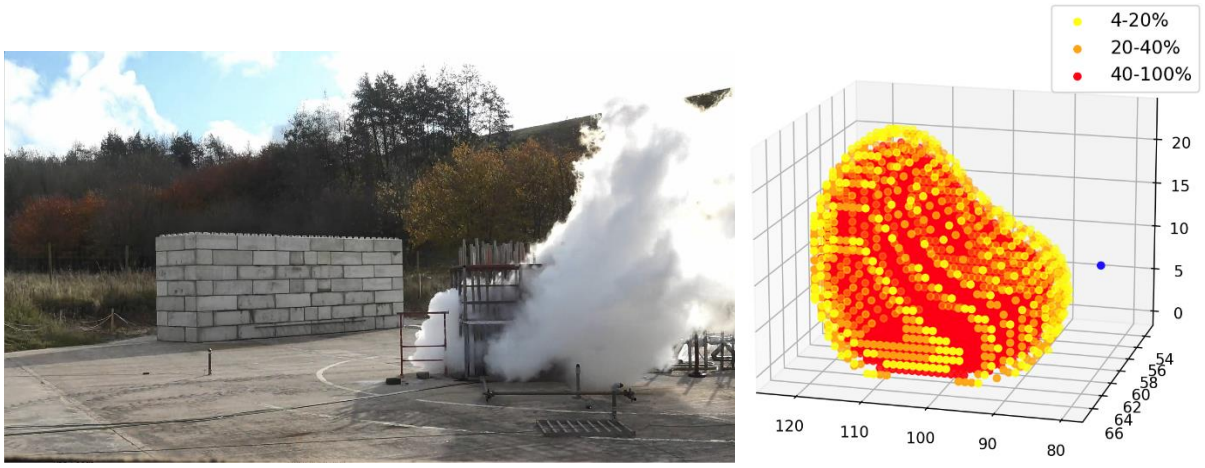

Figure 6: Photo and kriging plot of release event 23: high congestion, high counter flow wind

It is likely that the release jet and the low momentum dispersion would require separate variogram models as the two are governed by separate effects. Though the two may both be gaussian processes though they would likely require separate parameters (sill, range, and nugget). Additionally, to model the release jet with this methodology, comprehensive sensor points inside the jet stream including near and around the source would be necessary. Alternatively, it could be effective to combine this method with CFD simulation. Using CFD to model the release jet and kriging to model the low momentum wind dispersion could lower the computational cost compared to including real wind measurements in the CFD model.

Tuning the parameters of the gaussian process regression made significant impacts on the outcome of the model, indicating that the model is not very stable. There may exist a more informed variogram model that could be more resilient to variability, sensor error, and possibly describe both release jet and low momentum dispersion effects.

3.2 Explosion Severity Estimates

Table 4 shows the mass and explosion energy estimates of the hydrogen within the congestion frame for each test based on the visualizations using the kriging technique. The subset of experiments was selected based on at least 10 seconds of stable flow prior to ignition, to control the impact of outflow conditions on the results.

Table 4: Mass and blast energy estimates based on H2 concentration measurements and visualization regressions.

Test No.	Orifice (mm)	Storage pressure (kPa)	Blockage ratio (Volume %)	H2 mass estimate (g)	Blast energy estimate (MJ)
2	12	100	<1.5	193	23.2
3	25.4	100	<1.5	186	22.3
4	12	100	<1.5	162	19.5
5	25.4	100	<1.5	103	12.3
10	25.4	100	<1.5	133	16.0
15	12	500	<1.5	151	18.1
21	12	100	>4	181	21.7
23	12	100	>4	198	23.7

Based on the previous analysis [5], the energy of the severe event in test 23 was predicted to be in the range of 16 MJ to 27 MJ, with the other cases having a similar energy but less severity on the TNO level scale. The predictions based on the hydrogen concentration measurements fit within this estimated range, which lends credibility to quantitative nature of the visualizations. The more severe events also typically show a higher mass of hydrogen involved in the events: test 21 compared to 23 for the high level of congestion, and test 2 compared to 4 for the low level of congestion.

Table 5 shows the calculated *r'* values using equation 1, the measured peak overpressures at 6.5 m and 11.5 m, and the TNO level of the event. These results are graphically represented on figure 7, which is from the TNO Yellow Book [15].

Table 5: Scaled distances based on the mass estimates with the corresponding overpressure measurements and TNO level.

Test No.	**Overpressure at 6.5 m (kPa)**	**Overpressure at 11.5 m (kPa)**	**Calculated *r'* at 6.5 m**	**Calculated *r'* at 11.5 m**	**TNO Level**
2	4	2.3	1.05	1.85	3 to 4
3	0.5	0.4	1.06	1.88	1
4	1.2	0.7	1.11	1.96	2
5	1.1	0.5	1.29	2.29	2
10	0.4	0.2	1.18	2.10	1
15	4	2	1.14	2.01	3 to 4
21	4	2.5	1.07	1.89	3 to 4
23	47	20.5	1.04	1.84	8 to 10

Assessing the results displayed in Figure 7, the mass estimates result in energies that match the expected overpressure results for each event well, assuming the TNO level selected for each case is reasonable. It could be understood that the explosions were typically a TNO level 1-2 for a low-pressure release into the low level of congestion (tests 3, 4, 5, 10), with compounding factors such as higher release pressures (test 15) or higher congestion levels (test 21) resulting in a TNO level 3-4. In one case, test 2, the severity was a TNO level 3-4 without a compounding factor. This test was unique, however, in the sense that the peak overpressure was measured off-center. In all other tests the peak overpressure was measured at the center or rear of the congestion frame. While a higher mass of hydrogen was predicted within the frame, another potential cause of this behavior is that test 2 had the highest average windspeed (3.4 m/s compared to an average of 1.7 m/s) throughout the campaign and displayed an off-center cloud in the videos. The estimations of hydrogen mass show a slightly higher mass of hydrogen in the cloud, but the additional wind velocity could also have induced more turbulence, encouraging a more severe explosion.

The highest mass of hydrogen was predicted for test 23, which showed the largest TNO level. The next highest mass was in test 2, which also showed a higher severity than other tests with repeated initial conditions (test 4). With the relative closeness of the predicted masses (and therefore blast energies), the explosion severity is more likely to be a sperate factor, such as turbulence. Test 23 did have significant wind speed measurements in the moments leading up to ignition, which were not seen in the average data for that test. No direct measurements of turbulence were made, but the following features could have contributed to more turbulence within the congestion frame: higher storage pressure, more congestion, and greater magnitude or variability of the ambient wind conditions.

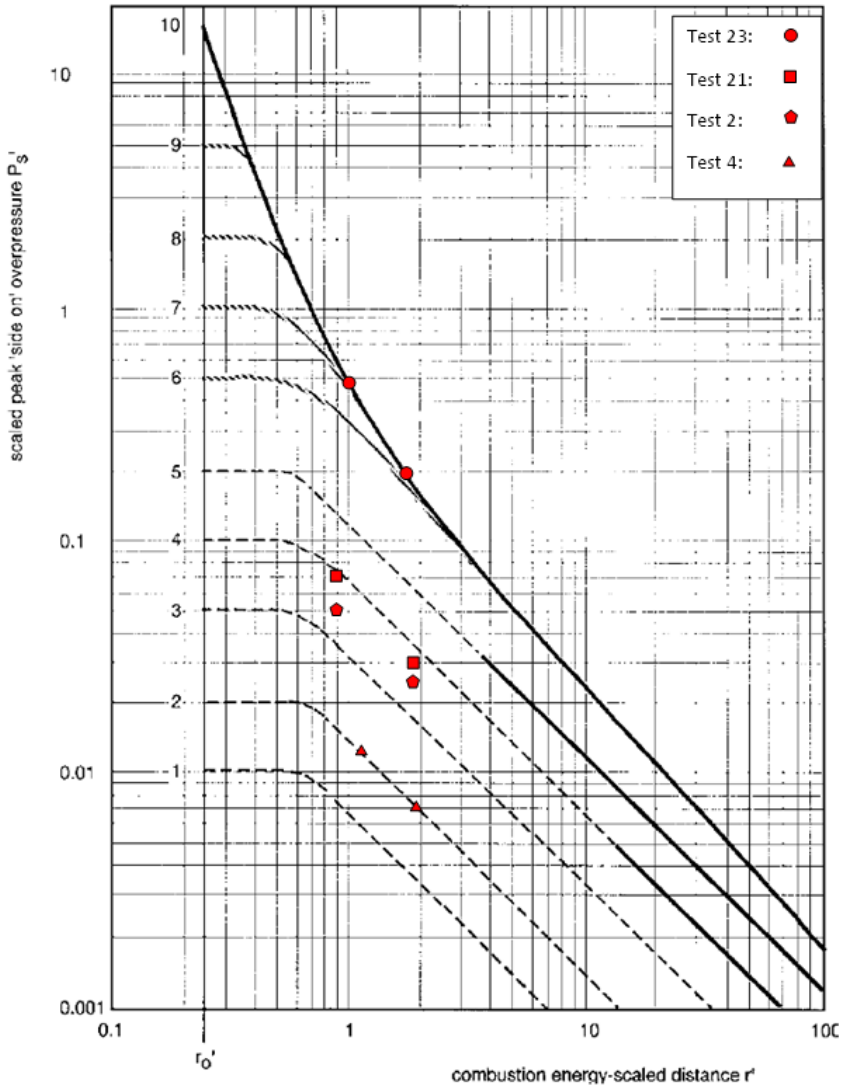

Figure 7: The Multi-Energy method blast chart: peak side-on overpressure including points for the measured overpressures and the scaled distance calculated using the mass estimates

4.0 CONCLUSION

Kriging, a machine learning interpolation technique, was used here to generate hydrogen mass estimates from isolated sensor points. The results were interpreted to establish relationships between wind, congestion, and explosive severity. Interpolation was performed by the National Renewable Energy Laboratory (NREL) on data generated in trials performed by the Health and Safety Executive (HSE).

Kriging was performed to find the concentrations at every point in space which was then plotted, confirming that the interpolation produced a reasonable representation of a gas plume. The kriging input parameters were tuned by seeking an optimally correlated data set according to the Spearman correlation method. Kriging produced volume percent estimates which were converted to total mass by using the ideal gas law. The pressure inside the gas cloud was assumed to be equal to the ambient pressure. Only gas within the congestion frame was summed because the turbulent gas inside the frame is the main contributor to explosive severity.

Allowing for variation in the TNO severity level, the mass estimates fall within the ranges expected to produce the explosion events that were witnessed. The largest events also typically showed a higher

mass contained within the congestion frame. However, the explosion severity could not be estimated based on the mass of hydrogen alone, as the energies were all relatively close at 16 MJ to 24 MJ. Compounding factors such as congestion, wind, and higher release pressures had a much larger amplifying effect on the measured overpressures than the relatively modest variation in estimated mass. The kriging interpolation method twined with the HyWAM sensors allows for a seemingly reasonable mass estimate, however difficulty remains in assigning the appropriate TNO severity level to allow for preemptive hazard assessments. The limited set of experimental data suggests that for a congestion level of < 1.5%, a TNO level 1 to 2 is typical, but could increase to a TNO level 3 to 4. For a congestion level of > 4%, a TNO level 3-4 is typical but could increase to a TNO level 8 to 10.

The use of kriging to describe gas clouds was shown to have both qualitative and quantitative applications. Qualitatively it was shown to produce plume shapes that were reasonably representative of the gas dispersion though the result lacked a representation of the high momentum release jet . Quantitatively it was shown that kriging can produce reasonable mass estimates that correlate to explosive characteristics and highlight the influence of wind and congestion, though the model was not stable with variation of input parameters. There may exist a variogram which would be more stable and capture both the high momentum jet stream and low momentum dispersion. Computational fluid dynamics could also be used to describe the high momentum release jet in conjunction with the use of kriging to interpolate the low momentum dispersion.

Further to this, the wider placement and dispersion of HyWAM sensors in congested or confined regions would lend more certainty to the quantitative estimates, and potentially lead to variations in both the visualized cloud shapes and the masses involved in the events. In order to capture the jet stream effects of the release, sensors would be needed in and around the jet stream, particularly near the release point. Additional types of sensors may also be beneficial such as oxygen sensors. Generally, the success of this type of analysis improves the more comprehensive (higher quantity and coverage of the congested area) the sensor deployment is.

ACKNOWLEDGEMENTS

This project has received funding from the Fuel Cells and Hydrogen 2 Joint Undertaking under the European Union's Horizon 2020 research and innovation programme under grant agreement No 779613. The HSE work programme acknowledges funding from its sponsors Shell, Lloyd's Register Foundation and Equinor and instrumentation provided by NREL and Dräger. The development and deployment of the NREL HyWAM was supported through the DOE Hydrogen and Fuel Cells Technology Office, Hydrogen Safety Codes and Standards Program. The contents of this paper, including any opinions and/or conclusions expressed, are those of the authors alone and do not necessarily reflect HSE policy.

REFERENCES

1. PRESLHY, Project Overview, accessed 22/03/2023, https://preslhy.eu/project-overview/
2. Verfondern, K. *et al.*, Handbook of hydrogen safety: Chapter on LH2 safety, PRESLHY, Rep. D6.1, 2021.
3. Houssin, D. *et al.*, Recommendations for RCS, PRESLHY, Rep. D6.3, 2021.
4. Hall, J.E. *et al.*, Characterisation, dispersion and electrostatic hazards of liquid hydrogen for the PRESLHY project, *Int. Conf. Hydrogen Safety*, Edinburgh (online), UK, 2021, pp. 1551-1563.
5. Lyons, K. *et al.*, Experimental parameters of ignited congestion experiments of liquid hydrogen in the PRESLHY project, *Int. Conf. Hydrogen Safety*, Edinburgh (online), UK, 2021, pp. 1420-1431.
6. Giannissi, S.G. *et al.*, CFD simulations of large scale LH2 dispersion in open environment, *Int. Conf. Hydrogen Safety*, Edinburgh (online), UK, 2021, pp. 49-59.
7. Buttner, W.J., Ciotti, M., Hartmann, K., Schmidt, K., Wright, H., and Weidner, E., "Empirical profiling of cold hydrogen plumes formed from venting of LH2 storage vessels," *Int. J. Hydrog. Energy*, 2018, doi: 10.1016/j.ijhydene.2018.10.231

8. Fuel Cell and Hydrogen Joint Undertaking, Project PRESLHY (Pre-Normative Research for Safe Use of Liquid Hydrogen), 2018. (see https://preslhy.eu/)
9. Buttner, W., Hall, J., Coldrick, S., Hooker, P., and Wischmeyer, T., "Hydrogen wide area monitoring of LH2 releases," *Int. J. Hydrog. Energy*, 46(23):12497–12510, 2021, doi: 10.1016/j.ijhydene.2020.08.266.
10. Buttner, W.J., Wischmeyer, T., Hall, J., Coldrick, S., Hooker, P., and Thorson, J., "'Hydrogen Wide Area Monitoring of LH2 Releases at HSE for the PRESHLY' Project (ID 153); Proceedings of the 2021 International Conference on Hydrogen Safety, Edinburgh, Scotland, 2021.
11. PRESLHY Work Package 3 (WP3) – Release and Mixing (see https://preslhy.eu/work-packages-2/wp3-release-and-mixing/), 2018.
12. PRESLHY Work Package 5 (WP5) – Combustion (see https://preslhy.eu/work-packages-2/wp5-combustion/), 2018.
13. Lyons, K., Summary of experimental series E5.5 (Congestion) results, PRESLHY, Rep. D5.7, 2021.
14. Lyons, K., PRESLHY experiment series E5.5, KIT open data, 2021, doi: 10.5445/IR/1000136285.
15. Van den Bosch, C.J.H. *et al.*, Methods for the calculation of physical effects due to releases of hazardous materials (liquids and gases) 'Yellow Book', TNO, CPR 14E, 2005.
16. N. Cressie, "The origins of kriging," *Math Geol* **22**, 239–252 (1990). https://doi.org/10.1007/BF00889887
17. C.A. Calder, N. Cressie, "Kriging and Variogram Models," *International Encyclopaedia of Human Geography, 49-55, (2009).* Kriging and Variogram Models - ScienceDirect
18. "Variogram Models – PyKrige 1.7.0 documentation," *geostat-framework.readthedocs.io.* Variogram Models — PyKrige 1.7.0 documentation (geostat-framework.readthedocs.io)
19. Interstate Technology Regulatory Council, "Perform Exploratory Data Analysis," *Geospatial Analysis for Optimization at Environmental Sites.* Perform Exploratory Data Analysis (itrcweb.org)